Scratch Modeling of Paint Coated Sheet Metal for Multi-Stage Deep Drawing Process

J Kim[1], J W Yoon[1,2*], B Lee[3], J Kim[3] and J Park[3]

[1] Department of Mechanical Engineering, Korea Advanced Institute of Science and Technology, 291 Daehak-ro, Yuseong-gu, Daejeon 34141, Republic of Korea
[2] School of Engineering, Deakin University, Geelong Waurn Ponds, VIC 3220, Australia
[3] Metal Forming Technology Team, Material & Production engineering Research Institute, LG Electronics, Jinwi-myeon, Pyeongtaek, Gyeonggi-do 17709, Republic of Korea

E-mail: j.yoon@kaist.ac.kr, j.yoon@deakin.edu.au

Abstract. The scratch phenomenon of paint coated sheet metal in multi-stage deep drawing has been investigated. The tensile tests at a quasi-static strain rate of sheet metals coated with two different types of paint were conducted along the rolling, diagonal, and transverse directions of the sheet metal in order to consider strain hardening and anisotropy. It has been found that the types of paint are negligible for plasticity behavior. Finite element simulations of the multi-stage deep drawing process was performed using the obtained material properties and the simulation results were compared with the actual testing. Through the simulation results, three approaches, which include the contact pressure, the accumulated slip distance, and the accumulated friction work were implemented to investigate the scratch phenomenon and they were compared for the scratched and non-scratched regions. It was found that the accumulated slip distance at the scratched region was larger than that of the non-scratched region with a good correlation from experimental observation, whereas either the contact pressure or accumulated friction work approach did not predict the experiments. Therefore, it is concluded that the accumulated slip distance is a good method to identify the scratch on the paint coated sheet metal during deep drawing process.

1. Introduction

Paint coated sheet metal (PCM) is widely used in home appliances, automobiles, etc., for corrosion prevention, aesthetics, and so on. In manufacturing products using PCM, it would be common to manufacture pre-coated materials for cost reduction. However, painting of the PCM may be separated from substrate during processes and it will cause additional waste and cost. Scratching of the coating is a process failure mode. A scratch is caused by the relative motion from mechanical contact between two solid bodies. In an effort to understand the scratch of the coatings, various scratch models have been proposed. The proposed scratch models were largely based on force or adhesion energy. As force-based scratch model, first, Benjamin and Weaver [1] suggested a scratch model based on the tangential force applied to materials. Critical shear stress, which is shear stress at the coating-substrate interface when the scratch initiates, can be obtained from the suggested model. In addition, they proposed a scratch model based on the normal force and this model can be also used to obtain the critical shear stress. Ollivier and Matthews [2] proposed a scratch model by modifying the work of Benjamin and Weaver [1]. Laugier [3] proposed a scratch model based on the total compressive stress acting at the leading edge of the indenter tip and the normal force, including friction effect and assuming elastic Hertzian contact. Besides the scratch models based on force, as an energy-based model, Laugier [4, 5] introduced the work of adhesion to describe the coating removal. In addition, both Bull et al. [6] and Attar and Johannesson [7] proposed scratch models which relate the critical load with adhesion energy including friction coefficient.

As mentioned above, the scratch behaviors are caused by the mechanical contact and the proposed scratch models are usually related to the force or energy. Thus, the objective of this study was to investigate the scratch phenomenon during multi-stage deep drawing by examining the parameters related to the force or energy during the contact, which are contact pressure, accumulated slip distance, and accumulated friction work, respectively. For this purpose, the tensile tests of the PCM material were conducted. After the tensile tests, finite element simulations of the multi-stage deep drawing process were performed. From the finite element analysis results, investigations on scratch phenomenon were carried out with the three approaches.

2. Tensile test at a quasi-static strain rate

To obtain the material properties of PCM, tensile tests at a quasi-static strain rate were conducted. The base material was SUS304 (BA). In addition, there were two types of paints which were coated to the sheet metal, one was Hi-Polymer (ARS) type and the other was soft feel type. To identify the differences in material properties between the two kinds of the PCMs, tensile specimens were prepared for each of the two types of PCMs. To consider anisotropy, specimens were prepared along the 0, 45, 90 degrees from the rolling. Specimen design was according to ASTM E8/E8M-16a [8] and detailed coating characteristics and specimen dimensions are summarized in Table 1 and Table 2.

Table 1. Coating characteristics for the PCMs.

Type	Hi-Polymer(ARS)	Soft feel
Coating system	Base(10 μm) + Top(10 μm)	Base(10 μm) + Clear(15 μm)
Color	Black	Black
Gloss	30%	5%

Table 2. Dimensions of the tensile specimen.

Parts	Dimensions (mm)
Overall length	38.45
Width	2.40
Thickness	0.30
Radius of fillet	12.18
Length of reduced parallel section	11.00
Length of grip section	9.60
Width of grip section	3.84

In order to identify the difference of the properties according to the types of PCMs during tensile testing, three tensile tests were performed by randomly selecting the test specimens for each type of PCMs. Table 3 shows the paint types of the specimens along the rolling, diagonal, and transverse directions used in the tensile test. Material testing has been conducted with and without coating. It has been found that there is no difference in the hardening behavior. So, the coating and interface effects have been ignored.

In the tensile test, the cross head speed of the test machine was set to 0.66 mm/min which maintains the strain rate of 0.001 /s and the strain was calculated using the Digital Image Correlation (DIC) method. Figure 1 shows engineering stress-strain curves for the rolling, diagonal, and transverse directions, respectively. From Figure 1, it has been shown that the stress-strain behaviors show the noticeable anisotropy for RD, DD and TD directions with very good repeatability within each direction.

Table 3. Paint types of the specimens.

	Rolling	Diagonal	Transverse
Specimen #1	Hi-Polymer(ARS)	Hi-Polymer(ARS)	Hi-Polymer(ARS)
Specimen #2	Soft feel	Soft feel	Hi-Polymer(ARS)
Specimen #3	Soft feel	Soft feel	Soft feel

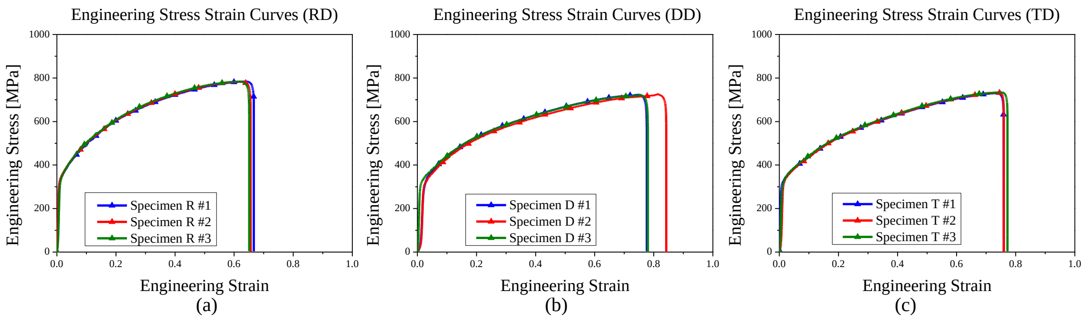

Figure 1. Engineering stress strain curves of PCMs: (a) rolling direction, (b) diagonal direction, (c) transverse direction.

Yield strength (YS), ultimate tensile strength (UTS), and r-value (Lankford's coefficient) for each direction of the PCM were calculated from the test and they are summarized in Table 4. To consider strain hardening behavior, Swift hardening model was assumed and its coefficients were calculated by fitting true stress-strain curve of specimen for the rolling direction. The Swift hardening model with the coefficients obtained from the test result is shown in Equation (1).

$$\sigma = 1{,}840\left(0.078 + \varepsilon_{\mathrm{p}}\right)^{0.709} \quad \text{(MPa)} \tag{1}$$

In addition, Hill's yield function [9] given by Equation (2) was used to model the anisotropic plastic behavior of the PCM. Coefficients, which are F, G, H, and N, were obtained from the average r-value shown in Table 4. The obtained coefficients were $F = 1.298$, $G = 1.034$, $H = 0.966$, and $N = 4.281$, respectively.

$$2\bar{\sigma}^2 = \left(G + H\right)\sigma_{11}^2 + \left(F + H\right)\sigma_{22}^2 - 2H\sigma_{11}\sigma_{22} + 2N\sigma_{12}^2 = 1 \tag{2}$$

Table 4. Yield strength, Ultimate tensile strength and r-value of the PCM.

	RD			DD			TD		
	YS (MPa)	UTS (MPa)	r-value	YS (MPa)	UTS (MPa)	r-value	YS (MPa)	UTS (MPa)	r-value
Specimen # 1	301.4	758.3	0.9280	271.4	695.4	1.318	293.6	726.3	0.7353
Specimen # 2	310.9	761.7	0.9381	286.1	703.1	1.283	315.3	737.5	0.7235
Specimen # 3	328.1	768.3	0.9348	303.5	696.5	1.406	305.0	721.5	0.7739
Average	313.5	762.8	0.9336	287.0	698.3	1.336	304.6	728.4	0.7442

3. Finite element simulation of multi-stage deep drawing

In order to investigate the scratch phenomenon of the PCM during the multi-stage deep drawing process, finite element analysis using the commercial finite element code Abaqus/Explicit was performed for the deep drawing processes. Figure 2 shows three dimensional model for deep drawing simulation and equivalent plastic strain distributions for each stage. In Figure 2(a), the parts shown in brown, blue, gray, and turquoise are blank, blank holder, punch, and die, respectively.

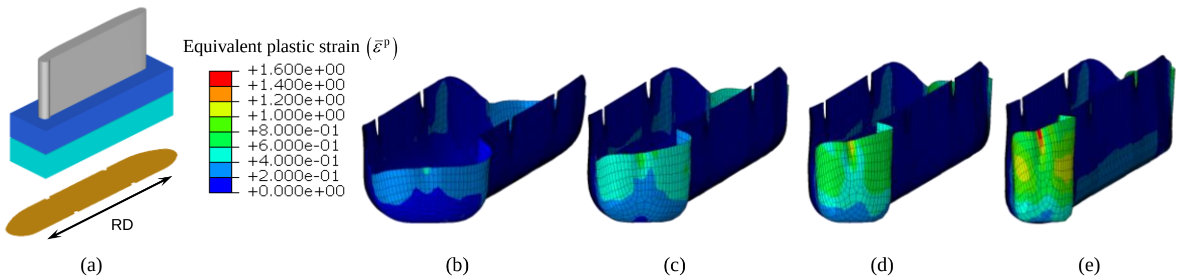

Figure 2. Three dimensional models for deep drawing process and equivalent plastic strain distributions for each stage: (a) all parts, (b) equivalent plastic strain distribution for 1st drawing, (c) for 2nd drawing, (d) for 3rd drawing, (e) for 4th drawing.

In this simulation, the parts except for the blank were modelled as a rigid body and the blank was modelled as deformable body where density, Young's modulus, and Poisson's ratio were 8,000 kg/m^3, 200 GPa, and 0.29, respectively. Plastic behavior was also modelled by using the strain hardening curve and yield function obtained from the tensile test given by Equation (1) and Equation (2).

In finite element modelling, the entire parts were discretized by finite element meshes. When generating the mesh system, 4-noded shell elements with reduced integration (S4R) was used for the blank. For other parts, 3-noded triangular and 4-noded quadrilateral rigid elements (R3D3, R3D4) were employed. As the boundary conditions, the blank holding force was 500 N and the punch speed was 200 mm/s. Normal contact and friction contact were also employed to model the contact between the blank and the tools. Coefficient of friction was tuned to be 0.01 in order to match the actual drawing height. In this FE models, interface models between the coating and the base metal were not implemented because the objective of this study was to investigate scratching using the parameters related to contact.

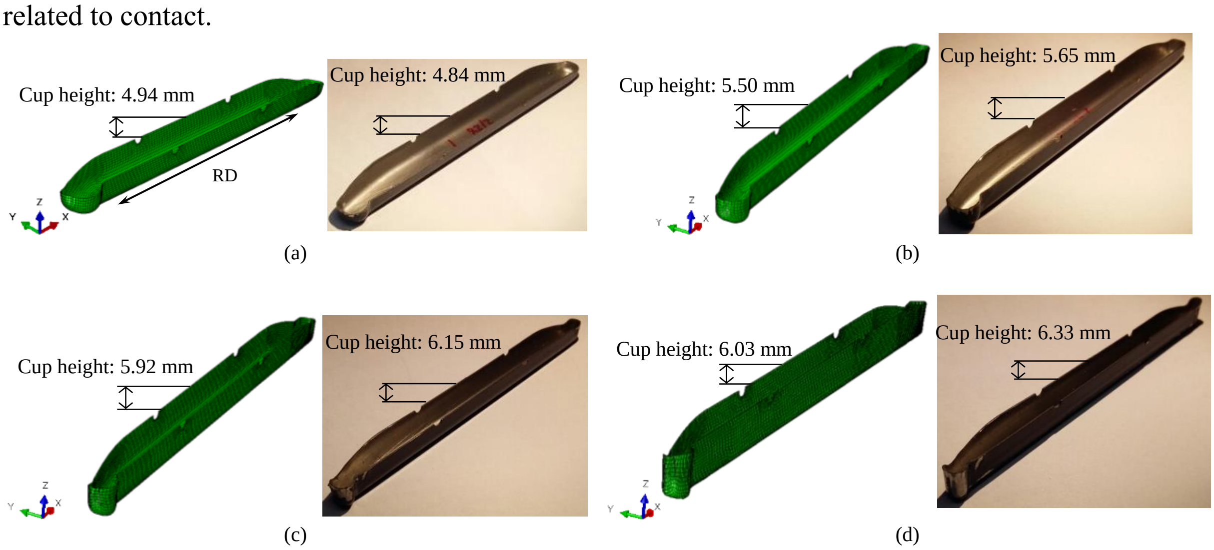

Figure 3. FE simulation results and actual drawing results for each drawing processes: (a) for 1st drawing, (b) for 2nd drawing, (c) for 3rd drawing, (d) for 4th drawing.

IOP Conf. Series: Materials Science and Engineering **418** (2018) 012100 doi:10.1088/1757-899X/418/1/012100

Figure 3 shows the actual drawing and simulation results of the FE model described in the above. As shown in Figure 3, the cup heights for each drawing process were close between the simulation results and the real products. These simulation results were used for the investigation of scratch phenomenon of PCM.

4. Investigation on scratch

As mentioned earlier, in order to investigate and model the scratch behavior of the PCM, the parameters related to the contact between the PCM and the tools were investigated. The parameters investigated in this study were the contact pressure, the accumulated slip distance, and the accumulated friction work, respectively. The investigation was conducted by observing scratched and non-scratched regions after each drawing process in the real products and calculating the parameters at the regions in the FEA results. Then, the calculated values in the scratched regions and the non-scratched regions were compared. In addition, in the investigation of the scratch of the PCM, the 2nd drawing were excluded because the experimental results were not stable. The detailed investigation results are described below.

4.1. Contact pressure

The contact pressure between the blank and the dies during each drawing processes were extracted from the analysis results to confirm the effect of the contact force on scratch. The maximum value of the contact pressure in the scratched and non-scratched regions were taken and compared. Figure 4 shows the maximum contact pressure distributions in the selected regions and the normalized drawing time at which it occurred with the views of the real products after each drawing. In Figure 4, a black line is the best line that distinguishes the scratched and non-scratched region and the region that appears silver in the real products is the peeled region. As shown in Figure 4, it was found that the maximum contact pressures difference between the scratched and non-scratched regions were not apparent for all drawing processes except for the 4th drawing. Thus, the maximum contact pressure would not be sufficient to model the scratch behavior of the PCM.

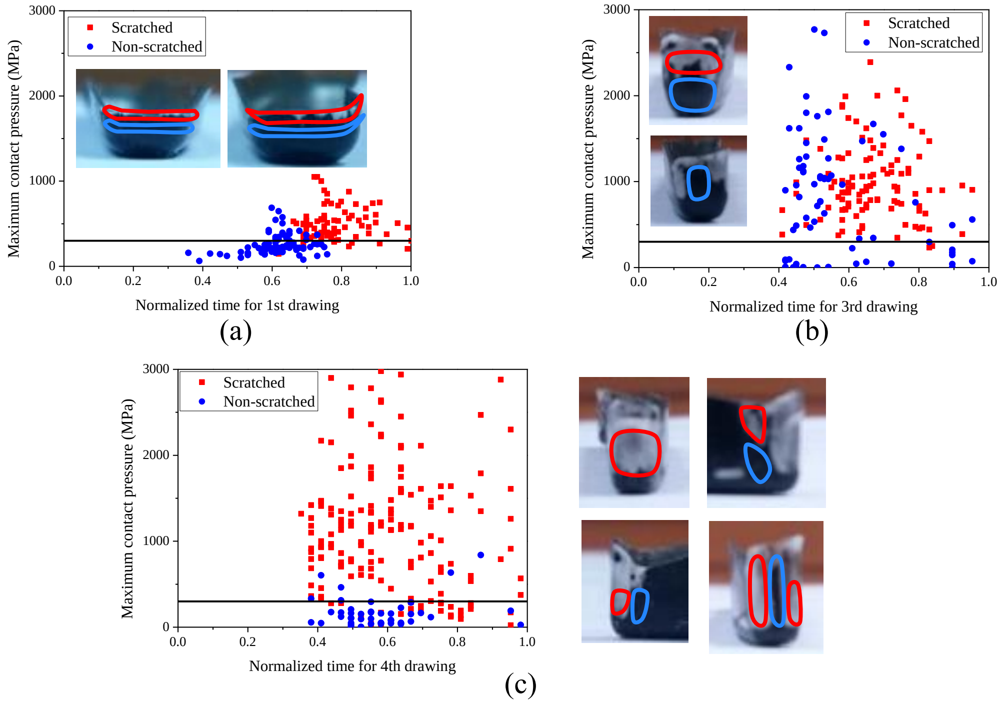

Figure 4. Maximum contact pressure distributions for each drawing processes (Red: scratched, Blue: non-scratched): (a) for 1st drawing, (b) for 3rd drawing, (c) for 4th drawing.

4.2. Accumulated slip distance and accumulated friction work

The objective of comparison of the accumulated slip distance was to confirm the effect of slip distance between the blank and the dies to the scratch. The method was similar to the comparison of the contact pressure: observing the scratched and non-scratched regions in the real products and calculating the accumulated slip distance at the selected regions from the FEA results. In this section, the word "accumulated" means summation from the 1st drawing to current drawing process. For example, the accumulated slip distance for the 3rd drawing process means the slip distance for the 1st drawing plus the one for the 2nd drawing plus the one for the 3rd drawing process at the selected region. Figure 5 shows the accumulated slip distance distributions for each drawing processes and a black line has the same meaning as the black line in Figure 4.

From Figure 5, it could be found that there were differences of the accumulated slip distances for the 1st drawing process at the scratched and non-scratched regions, i.e. the accumulated slip distance at the scratched regions were larger than that of the non-scratched regions. This tendency would also appear to have appeared in the 3rd and 4th drawing processes.

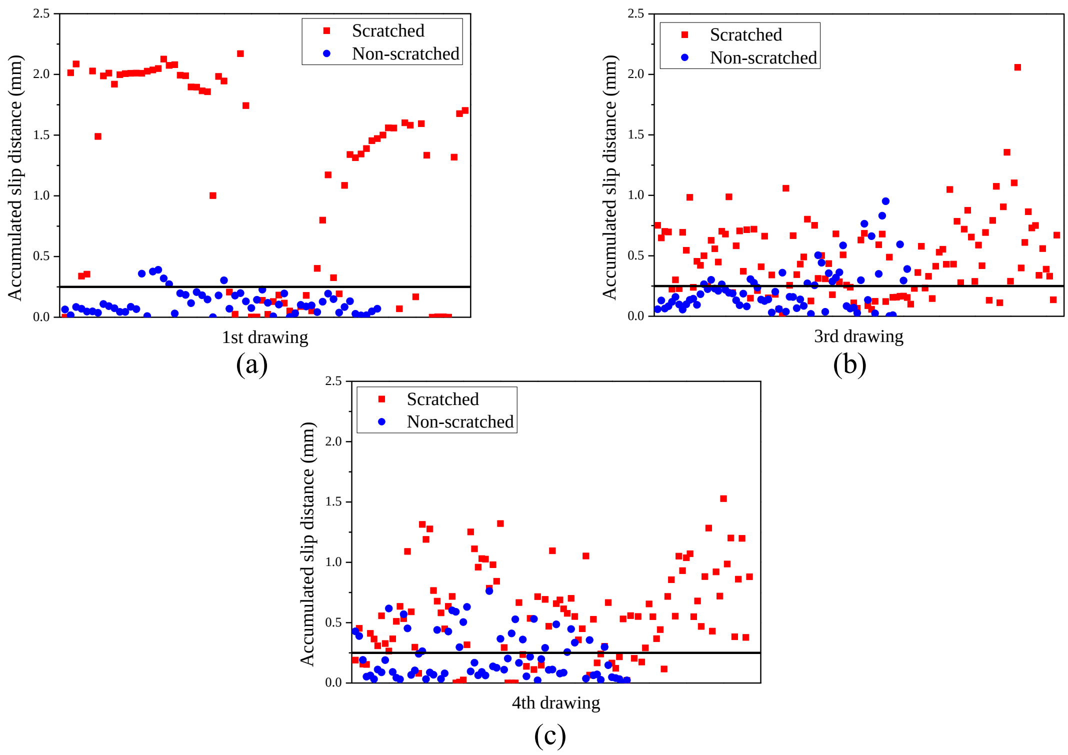

Figure 5. Accumulated slip distance distribution for each drawing process. (Red: scratched, Blue: non-scratched): (a) for 1st drawing, (b) for 3rd drawing, (c) for 4th drawing.

In addition to the accumulated slip distance, the accumulated friction work was calculated and compared. The accumulated friction work was calculated from Equation (3), using the contact force and the slip distance when the contact took place. In Equation (3), k means the drawing step, F_n, x, and μ mean the contact (normal) force, the slip distance, and the coefficient of friction, respectively. The word "accumulated" has the same meaning as the word described in the accumulated slip distance calculation. For example, the accumulated friction work for the 3rd drawing means the summation of friction work from 1st to 3rd drawing processes.

$$W = \sum_{n=1}^{k} \left(\int_{x_i}^{x_f} \mu F_n dx \right) \tag{3}$$

IOP Conf. Series: Materials Science and Engineering **418** (2018) 012100 doi:10.1088/1757-899X/418/1/012100

Figure 6 shows the accumulated friction work distributions at the selected regions calculated from Equation (3) and the best line that distinguishes the scratched and non-scratched region. As shown in Figure 6, the accumulated friction work at the scratched regions seemed to be larger than that of the non-scratched regions for all drawing processes.

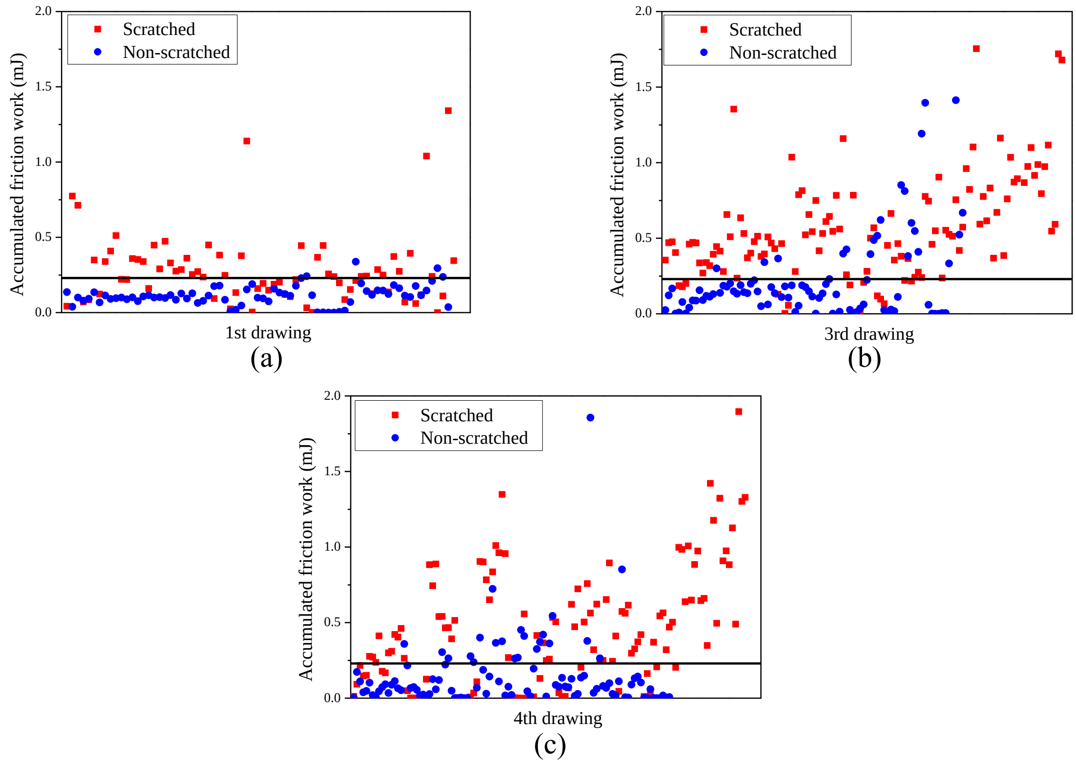

Figure 6. Accumulated friction work distributions for each drawing process. (Red: scratched, Blue: non-scratched): (a) for 1st drawing, (b) for 3rd drawing, (c) for 4th drawing.

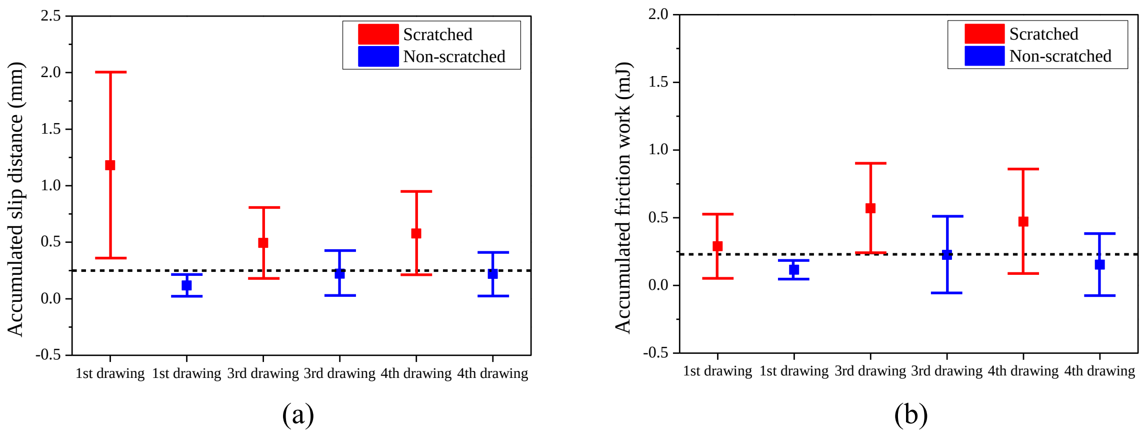

Figure 7. Accumulated slip distance and accumulated friction work distribution using mean and standard deviation: (a) accumulated slip distance, (b) accumulated friction work.

From the previous two results, it can be shown that there were the trends that the scratched regions have larger values of the accumulated slip distance and accumulated friction work than the non-scratched regions. To analyze the distribution of the parameters intensively, the mean and standard deviation were calculated. Figure 7 shows the distribution of each parameter using the mean and standard deviation. In Figure 7, when the mean value is m and the standard deviation is σ, the square box, upper bar, and lower bar mean m, $m+\sigma$, and $m-\sigma$, respectively.

From Figure 7, it was found that the accumulated slip distance distribution can be more clearly distinguished with the best dividing line, whereas the accumulated friction work has some violation. Thus, it could be found that the accumulated slip distance can explain the scratch behavior of the PCM and could be physically explained that the coating of the PCM would be scratched due to slip during the deep drawing processes.

5. Conclusion

In this study, the scratch phenomenon of the paint coated sheet metal during multi-stage deep drawing processes was investigated considering the contact pressure, the accumulated slip distance between the blank and dies, and the accumulated friction work. From the investigation results, it was found that the accumulated slip distance could distinguish the scratched and non-scratched regions while either maximum contact pressure or the accumulated friction work could not. Therefore, it is concluded that the accumulated slip distance can be used as a measure for estimating the regions susceptible to the scratch during deep drawing process.

References

[1] Benjamin P and Weaver C 1960 Measurement of adhesion of thin films. *Proceedings of the Royal Society of London A: Mathematical, Physical and Engineering Sciences*, **254**, pp. 163-176.

[2] Ollivier B and Matthews A 1994 Adhesion of diamond-like carbon films on polymers: an assessment of the validity of the scratch test technique applied to flexible substrates. *Journal of adhesion science and technology*, **8**, pp. 651-662.

[3] Laugier M 1981 The development of the scratch test technique for the determination of the adhesion of coatings. *Thin Solid Films*, **76**, pp. 289-294.

[4] Laugier M T 1984 An energy approach to the adhesion of coatings using the scratch test. *Thin Solid Films*, **117**, pp. 243-249.

[5] Laugier M 1986 Adhesion of TiC and TiN coatings prepared by chemical vapour deposition on WC-Co-based cemented carbides. *Journal of materials science*, **21**, pp. 2269-2272.

[6] Bull S J, Rickerby D S, Matthews A, Leyland A, Pace A R and Valli J 1988 The use of scratch adhesion testing for the determination of interfacial adhesion: The importance of frictional drag. *Surface and Coatings Technology*, **36**, pp. 503-517.

[7] Attar F and Johannesson T 1996 Adhesion evaluation of thin ceramic coatings on tool steel using the scratch testing technique. *Surface and Coatings Technology*, **78**, pp. 87-102.

[8] ASTM E8/E8M-16a 2016 *Standard Test Methods for Tension Testing of Metallic Materials* (Pennsylvania: ASTM International, West Conshohocken).

[9] Hill R 1998 *The mathematical theory of plasticity* (Oxford: Oxford university press).